Photodiagnosis and Photodynamic Therapy 28 (2019) 248–252

Contents lists available at ScienceDirect

Photodiagnosis and Photodynamic Therapy

journal homepage: www.elsevier.com/locate/pdpdt

Application of Raman spectroscopy in the detection of hepatitis B virus infection

Dongni Tong[a], Cheng Chen[b], JingJing Zhang[c], GuoDong Lv[d], Xiangxiang Zheng[b], Zhaoxia Zhang[a,*], Xiaoyi Lv[b,*]

[a] Department of Laboratory Medicine, The First Affiliated Hospital of Xinjiang Medical University, Urumuqi 83001, China
[b] College of Information Science and Engineering, Xinjiang University, Urumqi 830046, China
[c] Imaging Center, The First Affiliated Hospital of Xinjiang Medical University, Urumqi 830054, China
[d] State Key Laboratory of Pathogenesis, Prevention, and Treatment of Central Asian High Incidence Diseases, The First Affiliated Hospital of Xinjiang Medical University, Urumqi 830054, Xinjiang, China

ARTICLE INFO

Keywords:
Raman
HBV
serum
airPLS
PCA
SVM
Raman spectroscopy

ABSTRACT

Objective: Detection of hepatitis B virus (HBV) using Raman spectroscopy.
Methods: Raman spectroscopy was used to examine the serum samples of 500 patients with HBV and 500 non-HBV persons. First, the adaptive iterative weighted penalty least squares method (airPLS) was used to deduct the fluorescence background in Raman spectra. Then, a principal component analysis (PCA) was used to extract the processed Raman spectra, and a support vector machine (SVM) was used for modeling and prediction. The particle swarm optimization (PSO) algorithm was selected to optimize the parameters of the SVM instead of a traditional grid search. Finally, 600 serum samples were detected by Raman spectroscopy, and the results wereverified using a double-blind method.
Results: In the Raman spectra, the non-HBV human Raman peaks at 509, 957, 1002, 1153, 1260, 1512, 1648 and 2305 cm^{-1} were different from those of patients with HBV. The reported accuracy, sensitivity and specificity of the HBV serum model established using airPLS-PCA-PSO-SVM was 93.1%, 100% and 88%, respectively. The two groups were verified by a double-blind method. In the first group sensitivity was 87%, specificity was 92%, and the KAPPA value was 0.79; in the second group sensitivity was 80%, specificity was 79%, and the KAPPA value was 0.59.
Conclusion: This preliminary study shows that serum Raman spectroscopy combined with the airPLS-PCA-PSO-SVM model can be used for hepatitis B virus detection.

1. Introduction

Hepatitis B virus (HBV) infection is one of the most common causes of liver disease, from acute hepatitis to chronic hepatitis, which will progress to cirrhosis and hepatocellular carcinoma (HCC) [1]. Chronic hepatitis B is a global health problem affecting 350 million persons [2]. High HBV-DNA levels in serum are highly correlated with a high risk of HCC and cirrhosis in patients with chronic hepatitis B [3]. Since liver puncture is a traumatic examination method, serological plays an important role in the prevention, diagnosis and treatment of HBV infection. The enzyme-linked immunosorbent assay (ELISA) method is currently the most widely used detection method. The advantage is that the operation is simple and economical, and the disadvantage is that there are too many influencing factors. Real-time polymerase chain reaction (RT-PCR) is a method for detecting and quantifying HBV-DNA levels in clinical serum samples and can also be used to monitor antiviral treatment effects [4]. However, PCR is time consuming and requires specialized and expensive equipment. Therefore, it is of great practical significance to develop a more efficient, sensitive, and non-destructive diagnostic method.

Raman spectra are characterized by scattering [5]. Raman spectroscopy has evolved into a powerful analytical tool for providing important information about the combination of chemical structures and target analytes [6]. Raman spectroscopy samples do not require pretreatment, with the advantages of no damage detection and fingerprint resolution, and this technique is simple and fast [7]. Currently, Raman spectroscopy can be applied to the early diagnosis and identification of diseases. In terms of virus detection, Jin-Ho Lee et al. [8] successfully

* Corresponding authors.
E-mail addresses: 285715300@qq.com (Z. Zhang), xiaoz813@163.com (X. Lv).

https://doi.org/10.1016/j.pdpdt.2019.08.006
Received 1 May 2019; Received in revised form 28 July 2019; Accepted 2 August 2019
Available online 16 August 2019

measured HIV-1 VLP. S. Shanmukh et al. [9] distinguished respiratory syncytial virus strains. Khulla Naseer et al. [10] found that the Raman characteristic peak of plasma in patients with dengue is related to cholesterol specificity, indicating an increase in lipid content in the serum of patients with dengue virus infections. In terms of tumors, Sevda Mert et al. [11] concluded that Raman spectroscopy can be used to identify different tumor stages. Hong Wang et al. [12] concluded that Raman spectroscopy can effectively discriminate stage I, stage II or stage III/ IV serum samples from patients with nonsmall cell lung cancer. In cardiovascular terms, Nogueira et al. [13] adopted Raman spectroscopy to effectively distinguish nonatherosclerotic tissues, calcified atherosclerotic plaques, and calcified plaques.

Therefore, this experiment used Raman spectroscopy to detect the characteristic peak of HBV serum samples and explore its potential for screening HBV serum.

2. Materials and methods

2.1. Sample collection and preparation

A total of 1000 specimens were collected in the modeled experiments. Real-time PCR is a highly sensitive and reproducible method for the detection of HBV DNA. Therefore, this method was used to distinguish between the case group and the control group. There were 500 samples in the patient group. The patient group standard was HBsAg test positive, and the PCR results indicated that the HBV-DNA content was higher than the minimum detection limit in the fresh blood of patients with hepatitis B infections. The patient group exclusion criterion was blood with other infectious diseases. The other 500 samples were in the control group, and the inclusion standard was nonhepatitis B-infected fresh blood with an HBV-DNA content less than the minimum detection limit from PCR results, where suspected bacterial infection samples with serum PCT test results > 0.5 μg/L, type C hepatitis virus-positive patients, liver cirrhosis, liver cancer patients, and healthy persons were included. All patients were from the First Affiliated Hospital of Xinjiang Medical University. The 500 samples in the case group are shown in Table1.

In the test experiment, 600 serum samples were collected. Among these samples, 100 serum samples from the patient group were included in the first experimental group with the standard of HBsAg test-positive and hepatitis B virus-infected fresh blood with HBV-DNA content higher than the minimum detection limit by PCR. Another 100 serum samples were used as the control group with the standard of fresh blood from healthy individuals with negative serum antibodies in common infectious disease screening. In the second experimental group, the patient group included 200 serum samples with the standard of HBsAg test-positive and hepatitis B virus-infected fresh blood with HBV-DNA content higher than the minimum detection limit by PCR. Another 200 serum samples were used as the control group with the standard of nonhepatitis B-infected fresh blood with HBV-DNA content less than the minimum detection limit by PCR, where suspected bacterial infection samples with serum PCT test results > 0.5 μg/L, hepatitis C virus-positive patients, liver cirrhosis, liver cancer patients, and normal persons were included. All patients were from the First Affiliated Hospital of Xinjiang Medical University. The research project was approved by the Medical Ethics Committee of the First Affiliated Hospital of Xinjiang Medical University, and all specimens received informed consent from the patients.

Table 1
Clinical data of 500 case groups in the hepatitis B model.

Project	The number of cases
gender	
men/women	265(53%)/235(47%)
age	
< 50 / ≧50	314(62.8%)/ 186(37.2%)
hepatitis b virus DNA quantification	
< 105 / ≧105	286(57.2%)/ 214(48.2%)
immunoassay results	
(HBsAg+, HBeAg+, HBcAb+)/(HBsAg+, HBeAb+, HBcAb+)	415(83%)/85(17%)

All blood samples were collected in the morning after fasting for 12 h. The fresh blood was without any anticoagulant. To extract the serum, the blood samples were centrifuged at high speed (4000 r/min) for 20 min at 4 °C. Serum was obtained by extracting the supernatant from the uppermost layer, and the obtained serum was dispensed into a centrifuge tube and stored in a refrigerator at −20 °C for experimental use.

2.2. Raman spectrum acquisition

Fifteen microliters of each serum sample was pipetted. The serum Raman spectra were recorded by laser Raman spectroscopy (LabRAM HR Evolution RAMAN SPECTROMETER, HORIBA Scientific Ltd.) with a 50× objective lens at ambient temperature, and the spectral range was from 300 cm-1 to 3000 cm-1. The source was an Ar^+ laser with an excitation wavelength of 532 nm and power of 100 mW. Spectral data were obtained within 5 s, and a numerical aperture (NA) of 0.5 was used. Each sample was tested three times, and the average spectrum of each sample was further analyzed. A total of 1000 serum Raman spectra were obtained, of which 500 were from the case group and 500 were from the control group. In a double-blind trial, 600 serum samples were tested by a double-blind method.

2.3. Data analysis

2.3.1. Data preprocessing

The original Raman spectra contains significant fluorescence background and noise [14,15], which greatly affects the accuracy of the model analysis results. Therefore, it is necessary to select an appropriate preprocessing algorithm to subtract the fluorescent background and reduce its influence on the subsequent data analysis results. In this study, the airPLS algorithm was used, and the spectral data, after subtracting the fluorescent background, were normalized to eliminate noise interference and improve the convergence speed.

2.3.2. PCA feature extraction

If the preprocessed spectral data are directly classified, then the calculation amount will be too large. Therefore, it is necessary to extract the features. In this study, the preprocessed spectral data were extracted by PCA [16]. Three main components with the highest contribution rates, PC1, PC2 and PC3, were extracted. The constructed 3D scatter plot is shown in Fig. 1.

2.3.3. PSO-SVM modeling analysis

According to Fig. 1, the experimental group and the control group are mixed together and are difficult to distinguish by a conventional linear discriminant analysis algorithm. Based on the extracted features, 200 serum samples from the patient group and 200 serum samples from the control group were selected as the training set. A total of 300 serum samples from patients and 300 serum samples from the control group were selected as the test set, and the control group included suspected bacterial-infected samples with PCT test results > 0.5 μg/L, hepatitis C virus-positive patients, cirrhosis or liver cancer patients. The data for the training set and the test set were mapped into the high-dimensional space through SVM, and the optimal penalty factor c and the parameter g were searched by PSO to establish a suitable model. Then, the classification of the experimental group and the control group in the test set was completed.

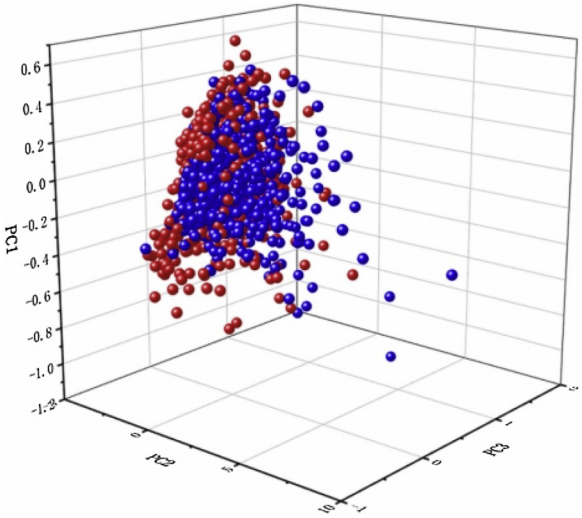

Fig. 1. Three-dimensional scatter plot of three principal components of Raman spectroscopy.

2.3.4. Test performance evaluation

After the double-blind test, the results were added to the four-grid table of the evaluation standard test (Table 2), and the sensitivity and specificity of the two sets of experiments were calculated. Sensitivity refers to the proportion of patients who test positive. Calculation formula: sensitivity = a / (a + c) × 100% Specificity refers to the proportion of individuals who have no disease in the test. Calculation formula: specificity = d / (b + d) × 100% Kappa value is a common indicator for evaluating the degree of conformity of the count data. Calculation formula: PA = (a + d)/n Pe = [(a + b)(a + c) + (c + b)(b + d)]/n2 K = PA-Pe/1-Pe

3. Results

3.1. Raman spectral analysis

As a kind of fingerprint, the serum Raman spectrum can indicate changes in biological molecules, such as proteins, nucleic acids and lipids, in different organisms and infer the physiological changes of the body to diagnose diseases. The spectra of 500 patient serum samples and 500 control serum samples were measured. The differences in Raman peaks are shown in Fig. 2A and B. At 509 cm^{-1}, 957 cm^{-1}, 1002 cm^{-1}, 1153 cm^{-1}, 1260 cm^{-1}, 1512 cm^{-1}, 1648 cm^{-1} and 2305 cm^{-1}, the Raman peak intensities of the control group are stronger than those of the case group. Table 2 shows the attribution of the characteristic peaks from the searched literature. HBV in the human body leads to biochemical changes in the serum, and the difference in the metabolism between amino acids and nucleic acids in the serum leads to the appearance of characteristic peaks in the Raman spectrum.

Table 2
Classification of the different Raman spectral peaks between control and case groups.

Peak	Assignment	Reference number
509 cm^{-1}	S—S disulfide stretching band of collagen	[19]
957 cm^{-1}	Hydroxyapatite, carotenoid, cholesterol	[20]
1002 cm^{-1}	Phenylalanine	[19]
1153 cm^{-1}	Carbohydrates peak for solutions	[21]
1260 cm^{-1}	Amide III (protein band)	[21]
1510 cm^{-1}	A (ring breathing modes in the DNA bases)	[22]
1647 cm^{-1}	Random coils	[28]
2305 cm^{-1}	Region of the OH—NH—CH stretching vibrations	[29]

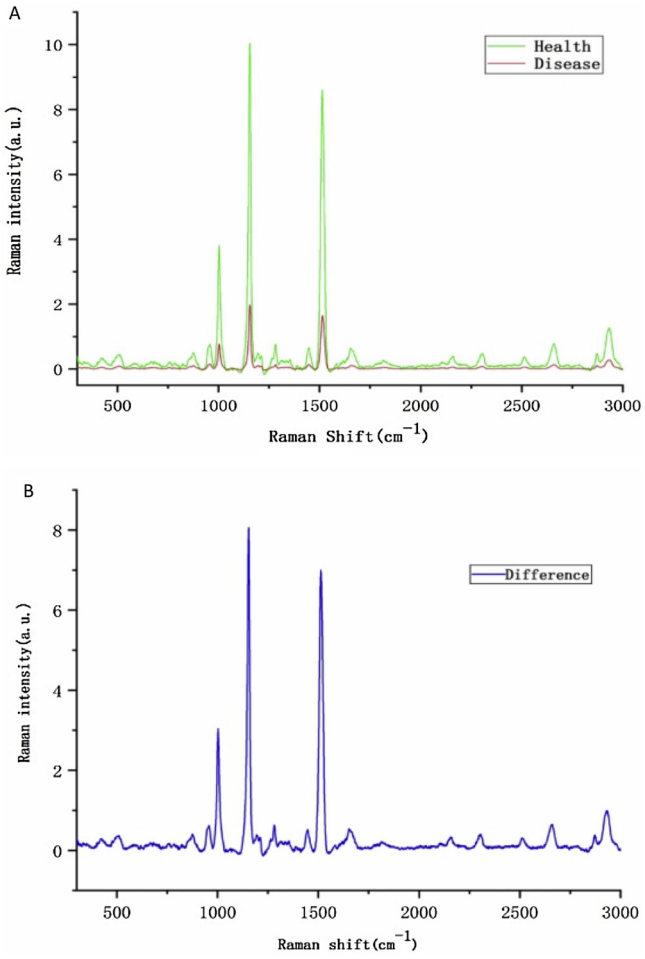

Fig. 2. A: Comparison of normalized mean Raman spectra between case and control groups. B: Differences in the peaks between case and control groups.

3.2. Data analysis

The preprocessed spectral data were processed by the PCA algorithm, and the feature extraction was performed by PCA. The three principal components with the highest contribution rates were selected, a three-dimensional scattergram was drawn, and the subsequent data were analyzed. The three-dimensional scattergram shows that it is difficult to distinguish between the experimental group and the control group by a conventional linear discriminant analysis algorithm. To complete the classification of the experimental group and the control group, this experiment selected a more powerful SVM and optimized the penalty factor c and the parameter g through PSO. In the training set, we selected 200 experimental group serum samples and 200 control group serum samples. In the test set, we selected 300 experimental group serum samples, 300 control group serum samples, and the control group included PCT test results > 0.5 μg / L suspected bacterial infection samples, hepatitis C virus-positive patients, cirrhosis or liver cancer patients and healthy human serum. The HBV-infected serum model established by PSO-SVM had an accuracy of 93.1%, a sensitivity of 100%, and a specificity of 88%.

To further validate the reliability of the model for the diagnosis of patients with hepatitis B virus, we plotted a receiver operating characteristic (ROC) curve as shown in Fig. 3. The area under the curve (AUC) was 0.942. The ROC curve combines the specificity and sensitivity of different models for the diagnosis of HBV-infected serum. AUC represents the diagnostic accuracy of the model, and a larger AUC value indicates a higher diagnostic accuracy [17].

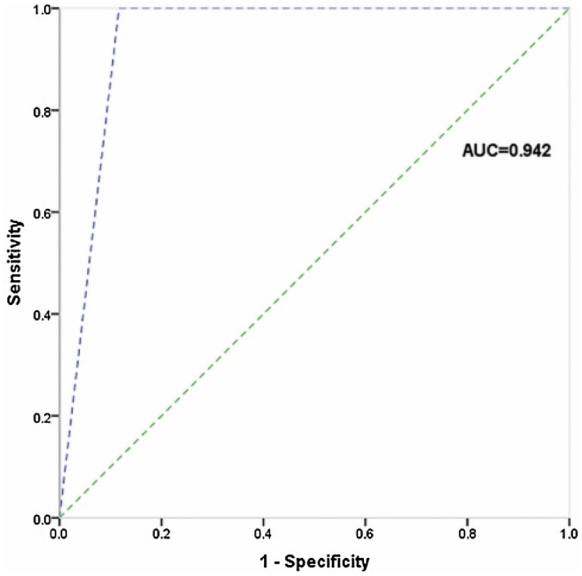

Fig. 3. ROC curve of the hepatitis B model established by PSO-SVM.

3.3. Test efficiency evaluation

In the first experimental group, 200 serum samples were detected by Raman spectroscopy using a double-blind method. The results are shown in Table 4. After calculation, we found that the sensitivity was 87%, the specificity was 92%, and the KAPPA value was 0.79. In the second experimental group, 400 serum samples were also examined by Raman spectroscopy using a double-blind method. The results are shown in Table 5. After calculation, we found that the sensitivity was 80%, the specificity was 79%, and the KAPPA value was 0.59.

4. Discussion

With the development of Raman spectroscopy for disease diagnosis, this technique been used to test proteins, nucleic acids, and proteins in different experimental materials, such as blood, saliva, urine, prostatic fluid, and tumor tissues, to obtain the characteristic Raman peaks of the diseases. After Raman scattering enhancement, background subtraction, linear discriminant analysis, and principal component analysis, fingerprint spectra for specific diseases can be generated, with strong sensitivity, specificity, and clinical significance.

The results of this study indicate that the serum of HBV patients has multiple characteristic Raman peaks compared with normal human serum, which may be used as a clinical diagnostic method for HBV. We found that the Raman peaks of HBV serum samples were significantly different in intensity at 1002, 1153, 1260 and 1513 cm^{-1}, consistent with Ref [18]. A independent variable *t*-test was performed on the 500 intensity data of the patient group and the 500 intensity data of the control group (preprocessing all data). At 509 cm^{-1}, 957 cm^{-1}, 1002 cm^{-1}, 1260 cm^{-1} and 1648 cm^{-1} $P < 0.001$, this indicates a significant difference in spectral relative intensity between the patient group and the control group. A decrease in the intensity of the Raman peak at 509 cm^{-1} is due to an S—S disulfide stretching band, which is related to cystine [19]. Cystine can promote cell redox and make liver function strong. Decreased peak intensities showed liver dysfunction. The intensity of the Raman peak at 957 cm-1, assigned for cholesterol, was also decreased [20]. When the liver develops severe lesions, the cholesterol concentration decreases. The Raman band at 1002 cm-1 could be assigned to the phenylalanine present in the serum albumin [19]. A decrease in the intensities of these peaks suggests a reduced concentration of albumin in the blood of an HBV-infected person. A depressed level of phenylalanine is most likely due to liver dysfunction in HBV-infected patients. The spectral features associated with proteins include those at 1260 cm-1 (amide III) and have lower intensity in HBV-infected blood plasma samples than in samples from healthy volunteers [21]. HBV is a DNA virus of the *Hepadnaviridae* family of viruses. The Raman peak at 1510 cm-1 is mainly due to the ring breathing mode of the DNA bases [22]. These characteristic peaks correspond to amino acids, cholesterol and proteins, and their content is reduced due to liver dysfunction. Therefore, we believe that Raman spectroscopy has potential advantages over other optical methods due to its ability to provide biochemical fingerprints.

Currently, in clinical practice, ELISA is still the main method for detecting serological markers of HBV, and the sensitivity of this method can reach (0.05–0.5) ng/mL [23]. With the development of nucleic acid detection technology, a fluorescent quantitative PCR method with high sensitivity, good specificity and a short window period has also been widely used in clinical practice, and its detection sensitivity can reach the order of 103 copies/ml [24]. Raman spectroscopy combined with airPLS-PCA-PSO-SVM was used to establish an HBV-infected serum model with an accuracy of 93.1%, sensitivity of 100%, and specificity of 88%. Although ELISA has the characteristics of simple operation and low price, its tests not only produce false-negative and false-positive results but are also time consuming. The sensitivity and specificity of real-time PCR depends mainly on the kit and the operation process. The Ministry of Health requires that the PCR laboratory be certified [25]. Raman spectroscopy has the characteristics of simple operation, time savings and high sensitivity.

In previous experiments [18], Raman spectroscopy was used to identify the characteristic peaks of HBV-infected serum, but only the difference between the Raman spectra of healthy people and patients was artificially distinguished. However, there was a large error, the sample set size was small, and the analysis result was easily affected by the contingency of the samples. Moreover, the noninfected samples selected by the previous experiment were healthy persons without any disease. According to the above problems, this experiment selected 500 patients with HBV and 500 persons without hepatitis B virus (including liver cancer, cirrhosis, hepatitis C virus patients, etc.) for modeling to fully evaluate the Raman spectroscopy diagnosis of hepatitis B virus. Finally, a double-blind experiment was conducted to further evaluate the performance of Raman spectroscopy in the diagnosis of hepatitis B virus.

The experimental results show that the airPLS-PCA-PSO-SVM model has very good sensitivity and specificity for the diagnosis of HBV-infected serum. AirPLS uses preprocessing of the data to maintain the original spectral peak shape, effectively deducting the fluorescent background in the Raman spectrum. Feature extraction is then performed using PCA, reducing the high dimensionality of the spectral data. If full-spectrum data are directly added as a variable to the SVM, the amount of calculation will be large, and all data may not be useful for modeling. Therefore, it is a good choice to quickly diagnose HBV-infected serum by Raman spectroscopy combined with multivariate statistical algorithms. However, in the current study, no experimental results showed that the appearance of Raman characteristic peaks is due to viruses or certain antigens and antibodies, which needs further research to verify. Gaggini MC et al. [26] considered that the Raman characteristic peaks of the liver from HCV patients were associated with the stage of the liver lesions, and biomarkers associated with the inflammation and/or fibrosis stages were found. Kun Zhang et al. [27] used serum Raman spectroscopy to distinguish liver cancer and cirrhosis patients from healthy individuals, and liver cancer screening could be realized. Therefore, we used 200 HBV patients as the experimental group and randomly selected 60 patients that were not infected with HBV but with cirrhosis or liver cancer, 30 patients that were not infected with HBV but were infected with HCV, and another 110 healthy persons as the control group. The double-blind experiment based on the model we designed was performed. The statistical results show that patients with HBV can be distinguished by Raman

Table 3
Evaluation standard four-grid table.

Raman spectroscopy	Gold standard		Total
	Positive	Negative	
Positive	a(True positive)	b(False positive)	a + b
Negative	c(False negative)	d(True negative)	c + d
Total	a + c	b + d	a + b+c + d

Table 4
Double-blind experimental results for the first experimental group.

Raman spectroscopy	Gold standard		Total
	Positive	Negative	
Positive	87	8	95
Negative	13	92	105
Total	100	100	200

Table 5
Double-blind experimental results for the second experimental group.

Raman spectroscopy	Gold standard		Total
	Positive	Negative	
Positive	160	42	202
Negative	40	158	198
Total	200	200	400

spectroscopy.

However, the sensitivity and specificity of the second group were lower than those of the first group (Tables 3 and 4), indicating that patients with other diseases may have similar Raman peak characteristics as the patients with HBV, which remains to be further improved.

5. Conclusion

This study demonstrates the use of Raman spectroscopy combined with the airPLS-PCA-PSO-SVM model to distinguish patients with HBV from healthy individuals, with an assay time below 20 min. Thus, HBV test results are reported as soon as possible to avoid misdiagnosis. The accuracy of the HBV model established using airPLS-PCA-PSO-SVM was 93.1%, the sensitivity was 100%, and the specificity was 88%. HBV can be effectively and rapidly determined by Raman scattering combined with the airPLS-PCA-PSO-SVM model. Raman spectroscopy is simple, objective, rapid, in real-time and highly sensitive, especially for the early diagnosis of diseases without clinical symptoms. Therefore, Raman spectroscopy combined with statistics has great potential for medical diagnosis.

References

[1] B. Wu, F. Xiao, P. Li, et al., Ultrasensitive detection of serum hepatitis B virus by coupling ultrafiltration DNA extraction with real-time PCR, PLoS One 12 (2) (2017) e0170290.

[2] G.L. Wong, V.W. Wong, H.L. Chan, Virus and host testing to manage chronic hepatitis B, Clin. Infect. Dis. 62 (Suppl. 4) (2016) S298–305.

[3] G.A. Kim, Y.S. Lim, S. Han, et al., High risk of hepatocellular carcinoma and death in patients with immune-tolerant-phase chronic hepatitis B, Gut 67 (5) (2018) 945–952.

[4] R.W. Chen, H. Piiparinen, M. Seppänen, P. Koskela, S. Sarna, M. Lappalainen, Real-time PCR for detection and quantitation of hepatitis B virus DNA, J. Med. Virol. 65 (2) (2001) 250–256.

[5] E.V. Efremov, F. Ariese, C. Gooijer, Achievements in resonance Raman spectroscopy review of a technique with a distinct analytical chemistry potential, Anal. Chim. Acta 606 (2) (2008) 119–134.

[6] R. Panneerselvam, G.K. Liu, Y.H. Wang, et al., Surface-enhanced Raman spectroscopy: bottlenecks and future directions, Chem. Commun. (Camb.) 54 (1) (2017) 10–25.

[7] M.B. Roeffaers, X. Zhang, C.W. Freudiger, et al., Label-free imaging of biomolecules in food products using stimulated Raman microscopy, J. Biomed. Opt. 16 (2) (2011) 021118.

[8] J.H. Lee, B.C. Kim, B.K. Oh, J.W. Choi, Rapid and sensitive determination of HIV-1 virus based on surface enhanced Raman spectroscopy, J. Biomed. Nanotechnol. 11 (12) (2015) 2223–2230.

[9] S. Shanmukh, L. Jones, Y.P. Zhao, J.D. Driskell, R.A. Tripp, R.A. Dluhy, Identification and classification of respiratory syncytial virus (RSV) strains by surface-enhanced Raman spectroscopy and multivariate statistical techniques, Anal. Bioanal. Chem. 390 (6) (2008) 1551–1555.

[10] K. Naseer, A. Amin, M. Saleem, J. Qazi, Raman spectroscopy based differentiation of typhoid and dengue fever in infected human sera, Spectrochim. Acta A. Mol. Biomol. Spectrosc. 206 (2019) 197–201.

[11] S. Mert, E. Özbek, A. Ötünçtemur, M. Çulha, Kidney tumor staging using surface-enhanced Raman scattering, J. Biomed. Opt. 20 (4) (2015) 047002.

[12] H. Wang, S. Zhang, L. Wan, H. Sun, J. Tan, Q. Su, Screening and staging for non-small cell lung cancer by serum laser Raman spectroscopy, Spectrochim. Acta A. Mol. Biomol. Spectrosc. 201 (2018) 34–38.

[13] G.V. Nogueira, L. Silveira, A.A. Martin, et al., Raman spectroscopy study of atherosclerosis in human carotid artery, J. Biomed. Opt. 10 (3) (2005) 031117.

[14] S. Li, G. Chen, Y. Zhang, et al., Identification and characterization of colorectal cancer using Raman spectroscopy and feature selection techniques, Opt. Express 22 (21) (2014) 25895–25908.

[15] Xiaozhou Li, Tianyue Yang, Siqi Li, Deli Wang, Youtao Song, Kedong Yu, Different classification algorithms and serum surface enhanced Raman spectroscopy for noninvasive discrimination of gastric diseases, J. Raman Spectrosc. 47 (8) (2016).

[16] Campos João Luiz Elias, Miranda Hudson, Rabelo Cassiano, Applications of Raman spectroscopy in graphene-related materials and the development of parameterized PCA for large-scale data analysis, J. Raman Spetrosc. 49 (1) (2017).

[17] Yin Jingjing, Hao Yi, Samawi Hani, Rochani Haresh, Rank-based kernel estimation of the area under the ROC curve, Stat. Methodol. (36) (2016) 91–106.

[18] Shahzad Anwar, Shamaraz Firdous, Optical diagnostic of hepatitis B (HBV) and C (HCV) from human blood serum using Raman spectroscopy, Laser Phys. Lett. 12 (7) (2015).

[19] W.T. Cheng, M.T. Liu, H.N. Liu, S.Y. Lin, Micro-Raman spectroscopy used to identify and grade human skin pilomatrixoma, Microsc. Res. Tech. 68 (2) (2005) 75–79.

[20] N. Stone, C. Kendall, J. Smith, P. Crow, H. Barr, Raman spectroscopy for identification of epithelial cancers, Faraday Discuss. 126 (2004) 141–157 discussion 169–83.

[21] R.K. Dukor, Vibrational spectroscopy in the detection of cancer, Biomed. Appl. (5) (2002) 3335–3359.

[22] J.W. Chan, D.S. Taylor, T. Zwerdling, S.M. Lane, K. Ihara, T. Huser, Micro-Raman spectroscopy detects individual neoplastic and normal hematopoietic cells, Biophys. J. 90 (2) (2006) 648–656.

[23] Wei Huang, Wei Wei, Xiao Tian Shi, Tianlun Jiang, The analysis of the detection performance of nucleic acid testing and ELISA for HIV, HBV and HCB, Front. Lab. Med. 1 (4) (2017).

[24] B. Wu, F. Xiao, P. Li, et al., Ultrasensitive detection of serum hepatitis B virus by coupling ultrafiltration DNA extraction with real-time PCR, PLoS One 12 (2) (2017) e0170290.

[25] S.H. Aliyu, M.H. Aliyu, H.M. Salihu, S. Parmar, H. Jalal, M.D. Curran, Rapid detection and quantitation of hepatitis B virus DNA by real-time PCR using a new fluorescent (FRET) detection system, J. Clin. Virol. 30 (2) (2004) 191–195.

[26] M.C. Gaggini, R.S. Navarro, A.R. Stefanini, R.S. Sano, L. Silveira, Correlation between METAVIR scores and Raman spectroscopy in liver lesions induced by hepatitis C virus: a preliminary study, Lasers Med. Sci. 30 (4) (2015) 1347–1355.

[27] Kun Zhang, Chunyan Hao, Baoyuan Man, Chao Zhang, Cheng Yang, Mei Liu, Qianqian Peng, Chuansong Chen, Diagnosis of liver cancer based on tissue slice surface enhanced Raman spectroscopy and multivariate analysis, Vib. Spectrosc. (2018).

[28] L.R. Jyothi, V.B. Kartha, K.C. Murali, R. SJG, G. Ullas, D.P. Uma, Tissue Raman spectroscopy for the study of radiation damage: brain irradiation of mice, Radiat. Res. 157 (2) (2002) 175–182.

[29] L. Seballos, J.Z. Zhang, R. Sutphen, Surface-enhanced Raman scattering detection of lysophosphatidic acid, Anal. Bioanal. Chem. 383 (5) (2005) 763–767.